

A causal multifractal stochastic equation and its statistical properties

François G. Schmitt

CNRS, UMR ELICO, Station Marine, Université de Lille 1, BP 80, 62930 Wimereux, France, e-mail: francois.schmitt@univ-lille1.fr

Received: date / Revised version: date

Abstract. Multiplicative cascades have been introduced in turbulence to generate random or deterministic fields having intermittent values and long-range power-law correlations. Generally this is done using discrete construction rules leading to discrete cascades. Here a causal log-normal stochastic process is introduced; its multifractal properties are demonstrated together with other properties such as the composition rule for scale dependence and stochastic differential equations for time and scale evolutions. This multifractal stochastic process is continuous in scale ratio and in time. It has a simple generating equation and can be used to generate sequentially time series of any length.

PACS. 47.27.Jv High-Reynolds-number turbulence – 02.50.Ey Stochastic processes – 05.45.Df Fractals – 47.27.Eq Turbulence simulation and modeling

1 Introduction

Since their introduction in the fields of turbulence, geophysics and chaos theory, multifractals have been widely used in many fields of applied sciences, including turbulence, geophysics, precipitations, oceanography, high energy physics, astronomy, biology and finance. The main characteristics of multifractal models or data is to possess high variability on a wide range of time or space scales, associated to intermittent fluctuations and long-range power-law correlations. In this framework, many studies have been devoted to data analysis and discrete mathematical model constructions. More precisely, there is a dichotomy in the multifractal literature between, on the one hand, experimental results showing usually no characteristic scales in a scaling range between an outer and an inner scale, and on the other hand, discrete cascade models that are not stationary and are scaling only for discrete scales ratios. This is why continuous multifractal models are needed, and among them, multifractal stochastic processes: processes possessing multifractal statistics while depending on a continuous time parameter. Here we consider one such process, belonging to the generatic family of lognormal multifractals, while depending on a continuous time parameter. This process has a simple analytical expression, and is causal and 1D. We will discuss some of its properties, and confirm them using data analysis of a numerical simulation.

Below we first recall the basic framework of discrete cascades: their statistics and correlation properties. These properties are given as the definition of a multifractal cascade process, and are recovered for continuous causal pro-

cesses. In section 2, we discuss the continuous scale limit of discrete cascades, and provide explicitly a basic causal equation generating a multifractal stochastic process for log-normal multifractals. We explore their statistical properties, including correlations for the process and its logarithm, and provide differential forms in time and in scale space. A link with the Langevin equation for Markov cascades is presented. Section 3 presents a simulation of a discrete cascade and a time simulation for a multifractal continuous process, together with a data analysis which confirms the theoretical results for both simulations. Section 4 is devoted to concluding remarks. Some useful results in probability theory are recalled in the Appendices.

1.1 The generic example of multiplicative cascades in turbulence

We briefly recall here the classical framework of Richardson turbulent cascades, which can be considered as the generic example of cascades. For high Reynolds number turbulence, dissipative terms are negligible compared to the inertial terms of the Navier-Stokes equations, so that for the inertial range, there is a local energy transfer from large to small scales. This is the picture of Richardson's 1922 energy cascade [1], which was later formalized by Kolmogorov in 1941 [2], corresponding to the Komogorov-Obukhov $-5/3$ Fourier power spectrum for velocity fluctuations in the inertial range. This description has been found experimentally valid for mean fluctuations, and this general cascade framework for the inertial range is now well accepted. Nevertheless it was not able to take into

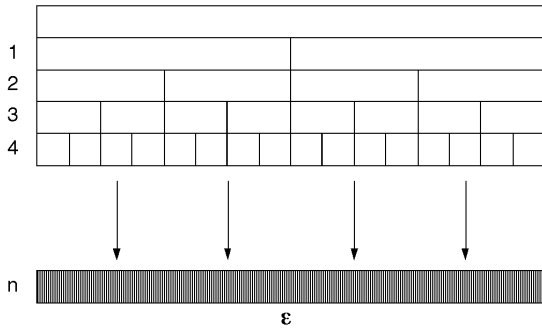


Fig. 1. Illustration of the discrete cascade process. Each step is associated to a scale ratio of 2. After n steps, the total scale ratio is 2^n .

account intermittent fluctuations of the small-scale dissipation field, as experimentally observed a few years later [3]. This intermittency lead Kolmogorov and Obukhov to propose new models in 1962 [4,5], assuming log-normal statistics for the velocity increments and for the dissipation field ϵ , with furthermore the following asymptotic hypothesis for the variance of $\log \epsilon$:

$$\sigma_{\log \epsilon}^2 \sim A + \mu \log \lambda \tag{1}$$

where A and $\mu > 0$ are constants (μ is often called the intermittency exponent), and $\lambda = L/\ell$ is the scale ratio of the outer scale L to the scale of interest ℓ (in the same paper this property of the variance was also assumed for the averaged dissipation ϵ_r , over a sphere of radius r). Kolmogorov’s proposals in 1962 were given without any physical or modelling justification; it was rather ad hoc. Soon after this, several experimental studies have shown that the dissipation field possesses long-range power-law correlations [6,7]. This was a very specific property which was not included in the proposal of Kolmogorov. This lead Yaglom to propose in 1966 his explicit cascade model, which was able to reproduce experimental facts – small-scale intermittency and power-law correlations – and the log-normal hypothesis of Kolmogorov. This multiplicative cascade model had hence experimental grounds, and was proposing an unification of different results and proposals. It is discussed below.

1.2 Discrete multiplicative cascades and their properties

We present now discrete multiplicative cascades and their statistical properties. This is basically a discrete model in scale, but it can be densified. The terms “discrete in scale” refer to the fact that the scale ratio from mother to daughter structures is an integer number strictly larger than 1. This model is multiplicative, and embedded in a recursive manner. The multiplicative hypothesis generates large fluctuations, and the embedding generates long-range correlations, that give to these large fluctuations their intermittent character.

1.2.1 Scaling properties of discrete multiplicative cascades

We symbolize the eddy cascade by cells, each cell being associated to a random variable W_i , called “weight”. All these random variables are assumed positive, independent, and identically distributed, with the following conservative property: $\langle W \rangle = 1$, where $\langle . \rangle$ denotes expectation. The larger scale corresponds to a unique cell of size $L = \ell_0 \lambda_1^n$, where ℓ_0 is a fixed scale and $\lambda_1 > 1$ is an adimensional scale ratio (very often for discrete models one takes $\lambda_1 = 2$). The model being discrete, the next scale involved corresponds to λ_1 cells, each of size $L/\lambda_1 = \ell_0 \lambda_1^{n-1}$. This is iterated and at step p ($1 \leq p \leq n$) there are λ_1^p cells, each of size $L/\lambda_1^p = \ell_0 \lambda_1^{n-p}$. There are n cascade steps, and at step n there are λ_1^n cells, each of size ℓ_0 , which is the smallest scale of the cascade (see Figure 1). To reach this scale, in agreement with Richardson’s original idea [1] and also with more recent results on the localness of interactions in turbulence [8], all intermediate scales have been involved. Finally, at each point the energy flux writes as the product of n weights [9]:

$$\epsilon(x) = \prod_{p=1}^n W_{p,x} \tag{2}$$

where $W_{p,x}$ is the random variable corresponding to position x and level p in the cascade. Since each $W_{p,x}$ for different cells are assumed independent, their moment of order $q > 0$ can be estimated as:

$$\langle (\epsilon(x))^q \rangle = \prod_{i=1}^n \langle (W_{p,x})^q \rangle = \langle W^q \rangle^n \tag{3}$$

Introducing the total scale ratio

$$\lambda = \frac{L}{\ell_0} = \lambda_1^n \tag{4}$$

between the outer and the inner scales, Eq. 3 gives finally the moments of the small-scale flux, denoted hereafter $\epsilon_\lambda(x)$ to indicate its scale-ratio dependence

$$\langle \epsilon_\lambda^q \rangle = \lambda^{K(q)} \tag{5}$$

where we introduced the cumulant generating function $K(q) = \log_{\lambda_1} \langle W^q \rangle$. The conservative property $\langle W \rangle = 1$ gives $K(1) = 0$ and also $\langle \epsilon \rangle = 1$.

Equation 5 is a generic property of multifractal fields, obtained through multiplicative cascades. Depending on the model chosen, different forms of the pdf of W can be taken, leading to different analytical expressions for $K(q)$. A log-normal pdf for W corresponds to a quadratic expression $K(q) = \frac{\mu}{2}(q^2 - q)$, with $\mu = K(2) = \sigma^2 / \log 2$, where σ^2 is the variance of $\log W$ (this is detailed below). It can be also noticed that $K(q)$ is (up to a $\log \lambda_1$ factor) the second Laplace characteristic function of the random variable $\log W$ (see the Appendix A), showing that it is a convex function (see [10]).

Let us mention here a specific property of multiplicative cascades: up to now, we have considered a cascading process from large to small scales, called “bare” field

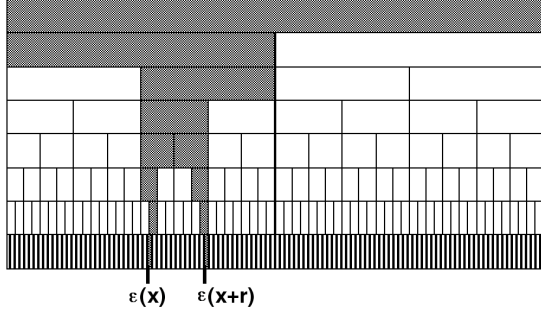


Fig. 2. The paths leading to 2 points separated by a distance r : they have a common path before a bifurcation.

by Mandelbrot [11], corresponding to the energy flux in turbulence. When the smallest scale is reached, the Kolmogorov dissipation scale η , the flux becomes the dissipation. An interesting question is here to characterize the “dressed” field, corresponding to integrated small-scale dissipation as proposed by Kolmogorov and Obukhov [4]. Dressed quantities (e.g. observables) are a measure, up to a resolution scale $r \gg \eta$, of the small-scale cascade, developed down to scale η . In fact, the dressing may introduce divergence of moments [11,18] but it is known that for moments below this critical moment q_D , the scaling exponents of bare and dressed fields are identical. An interesting mathematical question is also the convergence of the measure when the total scale ratio $\lambda = L/\eta \rightarrow \infty$ [12]. But this point is not the main topic of our paper. Indeed, the dressing is usually seen as performed by the observer; we therefore consider here our stochastic process (presented below) as representative of the cascade developed from a large to a smaller scale, i.e. a bare cascade. The question of the interrelation of dressed-bare fields and their respective statistical moments is therefore the same for our stochastic process, as for all multifractal cascade models (discrete or continuous).

1.2.2 Correlation properties

We now consider the long-range correlations generated by this cascade model. As originally shown by Yaglom [9], the correlation $\langle \epsilon_\lambda(x)\epsilon_\lambda(x+r) \rangle$ can be decomposed as a product of random variables, introducing their common ancestor as follows. The distance r corresponds in average to m steps, with $\lambda_1^m \approx r$, so that the $n-m$ first steps are common to the two random variables, whereas there is a “bifurcation” at the step m , and the two paths separate (see Figure 2). In the product of the two random variables, there are thus $n-m$ identical variables and m different and independent. This gives:

$$\begin{aligned} \langle \epsilon_\lambda(x)\epsilon_\lambda(x+r) \rangle &= \langle \prod_{p=1}^n W_{p,x} \prod_{p'=1}^n W_{p',x+r} \rangle \\ &= \prod_{p=1}^{n-m} \langle W_{p,x}^2 \rangle \prod_{p=n-m+1}^n \langle W_{p,x} \rangle \times \end{aligned}$$

$$\begin{aligned} &\times \prod_{p'=n-m+1}^n \langle W_{p',x+r} \rangle \\ &= \langle W^2 \rangle^{n-m} \langle W \rangle^{2m} \end{aligned} \quad (6)$$

Finally, introducing $K(q)$ and recalling that $\lambda_1^n = \lambda$ and $\lambda_1^m \approx r$ this gives:

$$\langle \epsilon_\lambda(x)\epsilon_\lambda(x+r) \rangle \approx \lambda^{K(2)} r^{-K(2)} \quad (7)$$

Since λ is fixed, this relation corresponds to a long-range power-law correlation with exponent $\mu = K(2)$. Let us note that the condition $\lambda_1^m \approx r$ imposes that the scaling relation (7) is exact for discrete scales only. This is an important limitation of discrete cascades, together with the fact that they are not strictly stationary. Relation (7) can be generalized to provide, following the same line, the two-points correlations of moments of order $p > 0$ and $q > 0$ [13,14]:

$$\langle \epsilon_\lambda(x)^p \epsilon_\lambda(x+r)^q \rangle \approx \lambda^{K(p+q)} r^{-(K(p+q)-K(p)-K(q))} \quad (8)$$

Since $K(q)$ is non-linear and convex for multifractal distributions, the exponent $K(p+q) - K(p) - K(q) > 0$ quantifies the long-range power law correlations of multifractal measures. For $p = q = 1$, this yields the $\mu = K(2)$ exponent given above.

On the other hand, we may also consider the correlation properties of the logarithm of the process (called generator), which possesses also interesting characteristics. Let us define the generators γ and g of respectively the cascade process ϵ and the weight W :

$$\begin{cases} \gamma = \log \epsilon \\ g = \log W \end{cases} \quad (9)$$

We consider the autocorrelation function of γ :

$$C_\gamma(r) = \langle \gamma(x)\gamma(x+r) \rangle \quad (10)$$

As before, the path leading to $\gamma(x)$ and $\gamma(x+r)$ may be split: for the last m steps the paths are different, whereas before this bifurcation, the paths are common. The main difference with the calculation leading to Eq.(7) is that in Eq. (10) γ is not the product but the sum of random variables. A simple calculation shows that $C_\gamma(r)$ involves $n^2 - n + m$ terms of the form $\langle g \rangle^2$ and $n - m$ terms of the form $\langle g^2 \rangle$. Let us note $G = \langle g \rangle = \langle \log W \rangle$ and $\sigma^2 = \langle (g - G)^2 \rangle = \langle g^2 \rangle - G^2$. We then have:

$$\begin{aligned} C_\gamma(r) &\approx \langle g \rangle^2 (n^2 - n + m) + \langle g^2 \rangle (n - m) \\ &\approx G^2 n^2 + \sigma^2 (n - m) \\ &\approx C - \frac{\sigma^2}{\log \lambda_1} \log r \end{aligned} \quad (11)$$

where we introduced the constant $C = G^2 n^2 + \sigma^2 n$. This corresponds to a logarithmic decay of the autocorrelation function of the generator [16,17]. Its Fourier transform gives the power spectrum of the singularity process $\gamma(x)$:

$$E_\gamma(k) \approx k^{-1} \quad (12)$$

corresponding to an exactly $1/f$ noise [18,19,20]. Properties (5), (8), (11) and (12) may be used to check the multifractality of a stochastic process. Analogous properties are verified for dressed multifractals and can hence be used to test numerical simulations or experimental data (for a link between log-correlations and dressed scaling properties, see also [20,21]).

1.2.3 The log-normal case

Up to now, the analytical expression taken by $K(q)$ is only loosely constrained a priori: a convex function verifying $K(0) = 0$ and $K(1) = 0$. We explicit here the generic example of multifractal cascade, given by the log-normal case, where generators are Gaussian. We choose here for simplicity $\lambda_1 = 2$. We take $W = e^g$, where g is a Gaussian random variable of mean G and variance σ^2 : $g = \sigma g_0 + G$, where g_0 is a centered and unitary Gaussian random variable. We have:

$$\langle W^q \rangle = \exp\left(\frac{1}{2}\sigma^2 q^2 + qG\right) \tag{13}$$

The conditions $\langle W \rangle = 1$ and $\mu = K(2) = \log_2 \langle W^2 \rangle$ provide the constants, and finally the weights of the form:

$$W = \exp\left(\sqrt{\mu \log 2} g_0 - \frac{\mu}{2} \log 2\right) \tag{14}$$

generate a discrete log-normal multifractal field with moment function

$$K(q) = \frac{\mu}{2} (q^2 - q) \tag{15}$$

This corresponds to log-normal statistics for ϵ , with a variance of $\log \epsilon$ obeying Kolmogorov’s initial hypothesis, given by Eq.(1). Formula (14) can be directly used for discrete log-normal simulations.

2 A causal log-normal stochastic evolution equation and its time and scale properties

2.1 Introduction

Up to now, a discrete cascade procedure has been presented, and its characteristic properties given. In this section we are interested in the scale densification, introducing more and more cascade steps, while maintaining constant the total scale ratio. We first recall below how this leads to log-infinitely divisible (log-ID) probability distributions. This considerably restricts possible pdf for continuous scale multifractal cascades. On the other hand, it is also very useful to have a stochastic equation generating continuous scale multifractal field or process at our disposal. Such a stochastic equation would depend on some parameters and a scale variable for fields, or on a time variable for processes. A few recent papers have been devoted to such topic, and we briefly present them below, before providing a stochastic equation corresponding to a causal log-normal multifractal process. We then study

this stochastic equation: we show that this produces indeed a multifractal log-normal process with the desired correlation properties, and we discuss further its differential form, when differentiated versus time and versus scale variables.

2.1.1 Continuous cascades lead to log-infinitely divisible processes and stochastic measures

To densify the cascade described above, we keep the total scale ratio λ large but fixed; the continuous limit can be obtained by increasing the total step number n , hence $\lambda_1 = \lambda^{1/n} \rightarrow 1^+$ (see [19,22,23,24]). It is then well-known that, in this limit, $\log \epsilon$ is an ID random variable (see Appendix A and [10] for ID random variables): continuous cascade models are log-ID [22,25,26,27]. This restricts the eligible cascade models, since ID laws define a specific family of probability distributions.

In order to provide stochastic equations and processes generating log-ID continuous multifractals, we have recently introduced ID stochastic integrals based on ID measures [28,29] (see also [30,31]). ID measures are set functions, also called in the mathematical literature independently scattered random measures [32]. This provided general expressions for the whole log-ID family. A more restricted but still quite general family is composed of log-stable processes, for which generating equations take simpler forms [18,14,29]. Among these, we consider here a special but important case: log-normal processes. We study this here because the stochastic integral involved is the classical Gaussian stochastic integral, whose statistical and differential properties are well-known; furthermore, log-normal multifractals are classical (and historical) examples of multifractals. The results given here for this type of continuous cascade may be generalized later for other ID processes.

Let us underline that the bare/dressed question mentioned above for discrete cascades is still valid for continuous cascades; the convergence properties of dressed log-ID measures has been studied in [30,33].

2.1.2 The stochastic equation

Until now, cascades have been presented in space; for the remaining of the paper, we consider cascades developing in time. The cascade is then seen as a stochastic process possessing long-range correlations for time increments τ .

The stochastic equation we study here is the following:

$$\epsilon_\lambda(t) = \lambda^{-\mu/2} \exp\left(\mu^{1/2} \int_{t+1-\lambda}^t (t+1-u)^{-1/2} dB(u)\right) \tag{16}$$

where $c > 0$ is a constant, $\lambda \gg 1$ is the total scale ratio, t is time and $B(t)$ is a Brownian motion. This was already given in [29] and in other less explicit forms in [18,19,14] but its statistical and differential properties have not been studied in details in these papers. This equation corresponds to the exponential of a Gaussian stochastic

integral, this integral being analogous to a fractional integration of a Gaussian process, i.e. a fractional Brownian motion [15]. The only difference with a formal fractional integration comes from the fact that the domain of integration is finite (for large values of λ it is a wide domain, but still finite). The exponent of this fractional Brownian motion is not a free parameter. Let us recall that for a self-similar parameter H the kernel in the integration for a fractional Brownian motion is on the form $(t-u)^{H-1/2}$, so that the kernel introduced above corresponds to a self-similar parameter $H = 0$. This is thus a very special case of fractional Brownian motion. This equation is also causal (the past does not depend on the future) and can be used to generate sequentially a log-normal process with no upper limit in the number of points. We study below in details the properties of this equation.

It is first easily verified that this process is stationary:

$$\epsilon_\lambda(t+t') \stackrel{d}{=} \epsilon_\lambda(t) \quad (17)$$

where $\stackrel{d}{=}$ means equality in distribution. The statistical moments are then independent of time, and are estimated below:

$$\begin{aligned} \langle \epsilon_\lambda(t)^q \rangle &= \lambda^{-q\mu/2} \langle e^{q\mu^{1/2} \int_{t+1-\lambda}^t (t+1-u)^{-1/2} dB(u)} \rangle \\ &= \lambda^{-q\mu/2} \exp\left(\frac{\mu q^2}{2} \int_{t+1-\lambda}^t \frac{du}{t+1-u}\right) \\ &= \lambda^{-q\mu/2} \lambda^{\frac{\mu q^2}{2}} \end{aligned} \quad (18)$$

giving the requested scale-invariant properties, Eq.(5) and Eq. (15) (see Appendix B for the second characteristic function of a stable stochastic integral). We explore below other properties of this equation in time and in scale-space.

2.2 Time statistics of the log-normal stochastic process

2.2.1 Correlations

We consider here the generalized correlation function

$$C_{\epsilon_\lambda}(p, q, \tau) = \langle \epsilon_\lambda(t)^p \epsilon_\lambda(t+\tau)^q \rangle \quad (19)$$

for moments of order $p > 0$, $q > 0$ and for $1 \leq \tau \leq \lambda$. The stochastic integrals are split in order to separate the overlapping integration domains, corresponding to independent random integrands. This gives:

$$\begin{aligned} C_{\epsilon_\lambda}(p, q, \tau) &= \lambda^{\frac{-\mu}{2}(p+q)} \times \\ &\times \langle \exp p\sqrt{\mu} \int_{t+1-\lambda}^{t+1+\tau-\lambda} (t+1-u)^{-1/2} dB(u) \rangle \\ &\times \langle \exp q\sqrt{\mu} \int_t^{t+\tau} (t+1+\tau-u)^{-1/2} dB(u) \rangle \end{aligned}$$

$$\begin{aligned} &\times \langle \exp \sqrt{\mu} \int_{t+1+\tau-\lambda}^t (p(t+1-u)^{-1/2} + \\ &+ q(t+1+\tau-u)^{-1/2}) dB(u) \rangle \\ &= I_1 \lambda^{\frac{-\mu}{2}(p+q)} \exp\left(\frac{p^2\mu}{2} \int_{t+1-\lambda}^{t+1+\tau-\lambda} \frac{du}{t+1-u}\right) \times \\ &\times \exp\left(\frac{q^2\mu}{2} \int_t^{t+\tau} \frac{du}{t+1+\tau-u}\right) \\ &= I_1 \lambda^{\frac{-\mu}{2}(p+q)} \left(\frac{\lambda}{\lambda-\tau}\right)^{\frac{p^2\mu}{2}} (\tau+1)^{\frac{q^2\mu}{2}} \end{aligned} \quad (20)$$

where I_1 is the last integral to evaluate:

$$\begin{aligned} I_1 &= \exp \frac{\mu}{2} \int_{t+1+\tau-\lambda}^t (p(t+1-u)^{-1/2} + \\ &+ q(t+1+\tau-u)^{-1/2})^2 \\ &= I_2 \exp\left(\frac{p^2\mu}{2} \int_{t+1+\tau-\lambda}^t \frac{du}{t+1-u}\right) \times \\ &\times \exp\left(\frac{q^2\mu}{2} \int_{t+1+\tau-\lambda}^t \frac{du}{t+1+\tau-u}\right) \\ &= I_2 (\lambda-\tau)^{\frac{p^2\mu}{2}} \left(\frac{\lambda}{\tau+1}\right)^{\frac{q^2\mu}{2}} \end{aligned} \quad (21)$$

with finally

$$\begin{aligned} I_2 &= \exp\left(\mu pq \int_{t+1+\tau-\lambda}^t \frac{du}{\sqrt{(t+1-u)(t+1+\tau-u)}}\right) \\ &= \left(\frac{\sqrt{\lambda-\tau} + \sqrt{\lambda}}{1 + \sqrt{\tau+1}}\right)^{2\mu pq} \end{aligned} \quad (22)$$

where we have used the identity

$$\int \frac{dx}{\sqrt{x(x+a)}} = 2 \log(\sqrt{x} + \sqrt{x+a}) \quad (23)$$

Eqs.(20), (21) and (22) give:

$$C_{\epsilon_\lambda}(p, q, \tau) = \lambda^{K(p)+K(q)} \left(\frac{\sqrt{\lambda-\tau} + \sqrt{\lambda}}{1 + \sqrt{\tau+1}}\right)^{k(p,q)} \quad (24)$$

with $k(p, q) = 2(K(p+q) - K(p) - K(q))$. Whenever $1 \ll \tau \ll \lambda$ this gives finally:

$$C_{\epsilon_\lambda}(p, q, \tau) \approx \lambda^{K(p+q)} \tau^{K(p)+K(q)-K(p+q)} \quad (25)$$

having the same asymptotic form as the generalized correlations for discrete cascades (Eq. (8)).

On the other hand, we may introduce the logarithm, called here singularity process

$$\begin{aligned} \gamma_\lambda(t) = \log \epsilon_\lambda(t) = & -\frac{\mu}{2} \log \lambda + \\ & + \mu^{1/2} \int_{t+1-\lambda}^t (t+1-u)^{-1/2} dB(u) \end{aligned} \quad (26)$$

and estimate its autocorrelation function for $1 \leq \tau \leq \lambda-1$ (using Appendix B):

$$\begin{aligned} C_{\gamma_\lambda}(\tau) = & \langle \gamma_\lambda(t) \gamma_\lambda(t+\tau) \rangle = \left(\frac{\mu}{2} \log \lambda \right)^2 + \\ & + \mu \left\langle \int_{t+1-\lambda}^t (t+1-u)^{-1/2} dB(u) \times \right. \\ & \left. \times \int_{t+1-\lambda+\tau}^{t+\tau} (t+1+\tau-u)^{-1/2} dB(u) \right\rangle \end{aligned} \quad (27)$$

As before, the stochastic integral can be split into two non-overlapping domains. Then, using Eq.(59) from Appendix B, we have:

$$\begin{aligned} C_{\gamma_\lambda}(\tau) = & \left(\frac{\mu}{2} \log \lambda \right)^2 + \mu \int_{t+1-\lambda+\tau}^t (t+1-u)^{-1/2} \times \\ & \times (t+1+\tau-u)^{-1/2} du \end{aligned} \quad (28)$$

and using again Eq.(23), this gives:

$$\begin{aligned} C_{\gamma_\lambda}(\tau) = & \left(\frac{\mu}{2} \log \lambda \right)^2 + 2\mu \log \frac{\sqrt{\lambda-\tau} + \sqrt{\lambda}}{1 + \sqrt{\tau+1}} \\ & \approx A_\lambda - \mu \log \tau \end{aligned} \quad (29)$$

where A_λ is a constant depending weakly on λ . The last line used as before the assumption $1 \ll \tau \ll \lambda$. Equation (29) is very close to Eq. (11) which was obtained for discrete cascades.

The stochastic process introduced in Eq. (16) has thus all the characteristic properties of multifractal cascades: multiscaling of the 1-point statistics, together with long-range power-law correlations for the process and log-correlations for the logarithm of the process. We consider below other properties of this equation: composition rules and differential forms.

2.2.2 Differential properties

Let us write stochastic equations for the processes $\epsilon_\lambda(t)$ and $\gamma_\lambda(t)$. First, let us consider the process $V_1(t) = \int_0^t (t+1-u)^{-1/2} dB(u)$. Applying the result given in Appendix B, $V(t)$ is a martingale process (with respect to the natural filtration) having the differential form:

$$\begin{cases} dV_1(t) = dB(t) + W_1(t)dt \\ W_1(t) = -\frac{1}{2} \int_0^t (t+1-u)^{-3/2} dB(u) \end{cases} \quad (30)$$

The same formula applied to the process $V_2(t) = \int_0^t (t+1-u)^{-1/2} dB(u)$ gives

$$\begin{cases} dV_2(t) = \lambda^{-1/2} dB(t) + W_2(t)dt \\ W_2(t) = -\frac{1}{2} \int_0^t (t+1-u)^{-3/2} dB(u) \end{cases} \quad (31)$$

These relations give then the stochastic process $\gamma_\lambda(t)$, having as differential form $d\gamma_\lambda(t) = \mu^{1/2}(dV_1(t) - dV_2(t+1-\lambda))$:

$$\begin{cases} d\gamma_\lambda(t) = \mu^{1/2} (dB(t) - \lambda^{-1/2} dB(t+1-\lambda)) - \frac{1}{2} W(t)dt \\ W(t) = \mu^{1/2} \int_{t+1-\lambda}^t (t+1-u)^{-3/2} dB(u) \end{cases} \quad (32)$$

For large scale ratios ($\lambda \gg 1$), the term $\lambda^{-1/2} dB(t+1-\lambda)$ may be neglected, since it is much smaller than $dB(t)$, so that the differential takes a simple form.

We consider now the stochastic differential equation for $\epsilon_\lambda(t) = \exp \gamma_\lambda(t)$. Ito stochastic calculus gives (recall that $dX(t) = X(t)dY(t) + \frac{1}{2}X(t)dt$ for $X(t) = \exp Y(t)$):

$$d\epsilon_\lambda(t) = \mu^{1/2} \epsilon_\lambda(t) \left(dB(t) + \frac{1}{2}(1 - W(t))dt \right) \quad (33)$$

where we have still neglected the term $\lambda^{-1/2} dB(t+1-\lambda)$, and $W(t)$ is given in Eq.(32). This provides the stochastic differential equation having as a solution the multifractal lognormal process studied here. It corresponds to a multiplicative process with a stochastic drift term. This may be compared to other families of stochastic differential equations; it can also be used for theoretical analyses, or to estimate (theoretically or numerically) the predictability properties of such processes. Indeed the long-range correlation properties of such process correspond to a long memory that can be exploited to optimize its predictability. This was already done in another context [14] and could be pushed further for the present stochastic process. We do not develop further this point here, and let such analysis for future studies.

2.3 Scale statistics of the log-normal stochastic process

In the previous section, we have considered the time properties of the stochastic evolution equation, for a given (and large) value of the scale ratio λ : time correlations and time stochastic differential equation. In this section we consider scale properties, assuming a fixed time t and considering the development of a cascade at a fixed point, when λ increases. We then define

$$E_t(\lambda) = \epsilon_\lambda(t) \quad (34)$$

We take λ as a continuous variable; in some instances we consider the log of the scale ratio and take as scale variable $\rho = \log \lambda$.

2.3.1 Semigroup composition properties

Let us first recall that, in consequence of their construction, discrete cascade, when considered at a fixed position, can be considered as a discrete Markov process in scale (see e. g. [34]): since successive multiplicative weights are independent, the product of $n + m$ weights can be decomposed into the product of n weights times the product of m weights, possessing a semi-group property.

We consider here a semigroup property hidden in our stochastic evolution equation.

$$\begin{aligned}
 E_t(\lambda_1 \lambda_2) &= (\lambda_1 \lambda_2)^{-\mu/2} \times \\
 &\times \exp \left(\mu^{1/2} \int_{t+1-\lambda_1 \lambda_2}^{t+1-\lambda_1} (t+1-u)^{-1/2} dB(u) \right) \\
 &\times \exp \left(\mu^{1/2} \int_{t+1-\lambda_1}^t (t+1-u)^{-1/2} dB(u) \right) \\
 &\stackrel{d}{=} E_t(\lambda_1) \lambda_2^{-\mu/2} \times \\
 &\times \exp \left(\mu^{1/2} \int_{t/\lambda_1-\lambda_2+1}^{t/\lambda_1} \lambda_1^{1/2} (t+\lambda_1(1-v))^{-1/2} dB(v) \right) \\
 &\stackrel{d}{=} E_t(\lambda_1) \exp \left(\mu^{1/2} \int_{t'+1-\lambda_2}^{t'} (t'+1-v)^{-1/2} dB(v) \right) \\
 &\stackrel{d}{=} E_t(\lambda_1) E_{\frac{t}{\lambda_1}}(\lambda_2) \tag{35}
 \end{aligned}$$

In the first equation the integration domain has been split in two non-overlapping domains, so that the corresponding random variables are independent. In the second equation, we have introduced a change of variable ($v-1 = \frac{u-1}{\lambda_1}$) and the fact that $dB(\lambda v) \stackrel{d}{=} \lambda^{1/2} dB(v)$. The third and fourth equations are simple factorizations (with $t' = \frac{t}{\lambda_1}$) using the definition of $E_t(\lambda)$. As a result, Eq.(35) is a decomposition property “in distribution”, for a fixed time.

Let us note that usually in papers studying Markov properties of the cascade in scale, the time or space variable do not appear. This is justified by the fact that the process is stationary, and that one often considers the probability instead of the process itself. To see this, let us introduce $\pi_\rho(x) = \Pr(\log E_t(e^\rho) = x)$. Then taking the log of Eq.(35), one obtains an equality in distribution for the sum of random variables, leading to a convolution of their probabilities:

$$\pi_{\rho_1+\rho_2} = \pi_{\rho_1} \otimes \pi_{\rho_2} \tag{36}$$

where $\rho_i = \log \lambda_i$.

This recovers the convolution semi-group property which can be found also in several recent papers [36, 27, 35]. In these papers, the convolution property has been shown to be directly linked to a decomposition property (originally introduced in [37]) of the pdf of the cascade process. This can also be obtained considering that the process

$f(\rho) = \log E_t(e^\rho)$ is a continuous Markov process with homogeneous transition probability of the form $Q_r(x, y) = \Pr(f(\rho+r) = y | f(\rho) = x) = q_r(y/x)$. Then Chapman-Kolmogorov equation for transition probabilities can be written on the following form

$$q_{r+s}(x) = \int q_r\left(\frac{x}{a}\right) q_s(a) da; \quad a > 0 \tag{37}$$

This equation is a general property of log-infinitely divisible (log-ID) processes, but since characteristic functions have simple expressions for such processes, it is often more convenient (as we do in the present paper) to characterize them using characteristic functions instead of probability distributions.

In a series of recent papers, Friedrich, Peinke and collaborators [40, 41, 42] have experimentally shown that, for a fixed position, the velocity or dissipation statistics in turbulence are Markov processes. Their Fokker-Planck approach can be shown to be linked (in case of lognormal cascades) to Castaing’s semi-group decomposition approach [38, 39, 36]. Below we consider in this framework different properties in scale, leading to a Langevin equation.

2.3.2 Differential properties and a Langevin equation

The series of papers about experimental evidence of a Markov process for the energy cascade in turbulence have considered either the velocity field or the dissipation field, and focused on a Fokker-Planck or Langevin (differential) equations (for a link between log-normal multifractal statistics and Fokker-Planck approach, see [38]). Here we give the theoretical expression obtained for our process and compare our result with experimental results published for the dissipation field in turbulence.

A stochastic (Langevin) equation has been obtained by Marcq and Naert [43] for the logarithm of the cascade process (more precisely the centered variable), involving the logarithmic scale ratio variable $\rho = \log \lambda$. We check here what this gives for our process. First for its generator, we have:

$$\begin{cases} \gamma_t(\rho) = \log \epsilon_\lambda(t) = -\frac{\mu}{2}\rho + \mu^{1/2} G(e^\rho) \\ G(x) = \int_{t+1-x}^t (t+1-u)^{-1/2} dB(u) \end{cases} \tag{38}$$

This is easily differentiated and provides:

$$\begin{cases} d\gamma_t(\rho) = -\frac{\mu}{2}d\rho + \mu^{1/2} e^\rho dG(e^\rho) \\ dG(x) = x^{-1/2} dB(t+1-x) \end{cases} \tag{39}$$

This may be more simply written introducing another Brownian motion $B_0(\lambda) = -B(t+1-\lambda)$ (recall that the time is frozen here), and writing the equation for the centered singularity $\gamma_0 = \gamma_t - \langle \gamma_t \rangle$:

$$d\gamma_0(\rho) = \sqrt{\mu e^\rho} dB_0(e^\rho) \tag{40}$$

where we used the property $\langle G(x) \rangle = 0$ and hence $\langle \gamma_t(\rho) \rangle = -\frac{\mu}{2}\rho$. For the process $E_t(\lambda)$ itself, this gives the

following equation:

$$dE_t(\lambda) = E_t(\lambda) \left(\frac{d\lambda}{2} \left(1 - \frac{\mu}{\lambda} \right) + \mu^{1/2} \lambda^{1/2} dB_0(\lambda) \right) \quad (41)$$

This gives the Langevin equation in scale for our continuous multifractal process (for a fixed time).

Our results can be compared to previous studies, some of them done in purely experimental grounds. Let us first note that in some cases (see [41]) the study is done considering a Fokker-Planck equation with drift and diffusion coefficients D_1 and D_2 . The associated stochastic differential equation (Langevin form) is:

$$d\gamma(\rho) = D_1(\rho)d\rho + \sqrt{2D_2(\rho)}dB(\rho) \quad (42)$$

so that our results given in Eq.(40) for the centered variable provide an equation analogous to Eq.(42) with:

$$\begin{cases} D_1(\rho) = 0 \\ D_2(\rho) = \frac{1}{2}\mu e^\rho \end{cases} \quad (43)$$

Our stochastic equation is thus analogous to a zero drift and scale-dependent diffusion coefficient, but with a subordinated Brownian motion $B_0(e^\rho)$, instead of the process itself. Let us underline that this applies to a bare cascade, developing from large to small scales, at a fixed time. This can be compared to the results given by Cleve and Greiner [34] for a discrete bare cascade, where they also find a zero drift coefficient. On the other hand, experimental results on the Markov property of the cascade correspond to properties of the dressed cascade and therefore may not be related directly to properties of the bare cascade. This difference was already underlined in [34] where it was shown numerically (from a discrete cascade simulation) that the dressing introduces a non-zero drift term. The theoretical reasons to obtain a Markov property for dressed quantities is also less straightforward than for bare ones. Nevertheless, we may compare the values given by our bare model with dressed experimental results. Naert et al. [41] have experimentally obtained a non-zero drift value and a constant D_2 ; later Marcq and Naert [43] have found a scale-dependent diffusion term of the form $D_2(\rho) = D_0 e^{2\delta\rho}$ with $D_0 \approx 0.01$ and $\delta \approx 0.4$. This is closer to our result: D_0 is clearly too small in [43] compared to our expression (recall that experimentally, μ is close to 0.25, leading to $D_0 \approx 0.12$) but the ρ -dependence is almost the same since we would have $\delta = 1/2$. In any case we do not expect here to recover the same values, since (i) there may be a bare-dressed difference in the coefficients and (ii) the discrepancy between our theoretical expression and experimental results are also likely to come from the fact that we took for simplicity (as a first step) a log-normal cascade here, whereas the real picture in turbulence seems to be more involved (see e.g. [44]).

Let us underline once more that this scale description is valid only for a fixed position in time or in space, since the long-range correlations of turbulence in time or in space are not compatible with a Markov process. A more complete representation of the cascade process is then –

as we do in the present paper – to provide a time-scale description. In this time-scale space, the process involved is more complex than being simply Markovian.

2.3.3 Interpretation of multiplicative cascades as stochastic continuous products

Discrete cascades correspond to a finite product of random variables. For convenience reasons, the densification has been interpreted above as the exponential of a stochastic integral. In fact, the natural way to densify the cascade would be to introduce more and more intermediate scales in the finite product, while keeping the total scale ratio fixed. This corresponds to a continuous product (for deterministic continuous products see [45]). Stochastic continuous products (also sometimes called stochastic multiplicative integrals) have been introduced by McKean [46], and developed by e.g. Ibero [47], Doleans-Dade [48] and Emery [49] in the framework of continuous martingales. As first argued in [28], continuous products are necessary when one needs to introduce zeroes (such as in a continuous generalization of the discrete β -model [50]), or when generalizing the 1D approach to matrix or tensorial cascades. Stochastic continuous products provide in fact an interesting mathematical framework to study continuous cascades, since some results obtained in this field may be applied to multifractal cascade processes. Some first results in this approach are given below.

Among the results obtained by Ibero [47] is the following: under general conditions on the square matrices functions f and e (they can be stochastic functions), the following multiplicative stochastic integral (denoted as \int , see Appendix C for a definition) is converging

$$z(t) = \int_0^t \exp(f(s)ds + e(s)dB(s)) \quad (44)$$

and is the solution of the following stochastic differential equation:

$$dz(t) = z(t) \left((f(t) + \frac{1}{2}e^2(t))dt + e(t)dB(t) \right) \quad (45)$$

in the algebra of square matrices of order n (B is a matrix Brownian motion). This framework is useful for cascades of matrices, which can be used to consider vectorial multifractal processes. In this line, the generalization of Eq.(16), is, introducing continuous product:

$$\epsilon_\lambda(t) = \lambda^{-\mu/2} \int_{t+1-\lambda}^t \exp\left(\mu^{1/2}(t+1-u)^{-1/2}dB(u)\right) \quad (46)$$

which will give an equation analogous to Eq. (33) for square matrices. Indeed, for 1D processes, this equation gives back Eq.(16), while for the general multi-dimensional case where B is a matrix Brownian motion, this stochastic continuous product can be shown to correspond to a matrix multifractal process. This means that each element of

such matrix is a 1D multifractal process, while they also possess two-by-two scaling properties. We do not explore further here the multifractal and correlation properties of Eq. (46); this will be done elsewhere. Nevertheless, it is clear that it would be interesting to develop such theoretical framework in order to perform data analysis, such as for example for analyzing multidimensional data series. We discuss here a potential application of such approach: these cascades of matrices may be used to model intermittent anisotropic tensors in turbulence, such as the dissipation rate $\epsilon_{ij}(t)$ where it is defined as

$$\epsilon_{ij} = 2\nu \left\langle \frac{\partial u_i}{\partial x_k} \frac{\partial u_j}{\partial x_k} \right\rangle \quad (47)$$

Indeed, according to Kolmogorov's 1941 hypothesis, for high Reynolds number flows the cascade process is assumed to "wash" the details of the large-scale flow so that after enough cascade steps the dissipation tensor becomes isotropic. In fact experimental results in homogeneous turbulence indicate that this may not be true [51]. Several deterministic closure models have been developed to take into account this anisotropy for homogeneous and non-homogeneous turbulence (see e.g. [52,53]). This type of model are fully tensorial and can be numerically solved to provide the prediction of some statistical quantities (such as mean and second moments of the velocity field). But they need too drastic hypothesis (in particular they are not compatible with the long-range correlation properties of turbulence) and they provide, at best, adequate predictions for moments up to order 2 (see a general presentation on this in [54]). On the other hand, turbulent cascade models are able to reproduce experimental fluctuations of the velocity field up to moments of order 7 (see [55]), but up to now they can deal only with 1D processes. Because of this limitation, they have offered until now very limited industrial applications. If turbulent cascade models could be adapted to vectorial or tensorial frameworks, it could, in a relatively short time, lead to much more reliable predictions for industrial flows. This promising research direction is not developed further here.

3 Simulations

We perform here numerical simulations of discrete and continuous cascades. The aim of these simulations is to check the theoretical relation given in previous sections, and to compare discrete and continuous cases.

3.1 Simulation of discrete log-normal cascades

We perform here a numerical simulation of a discrete log-normal cascade with $\lambda_1 = 2$ and weights given by Eq.(14). This is illustrated here with $n = 12$ cascade steps, corresponding to a total scale ratio of $\lambda = 2^{12} = 4096$, and a value of the intermittency parameter close to experimental results for the dissipation: $\mu = 0.25$. Figure 3 shows

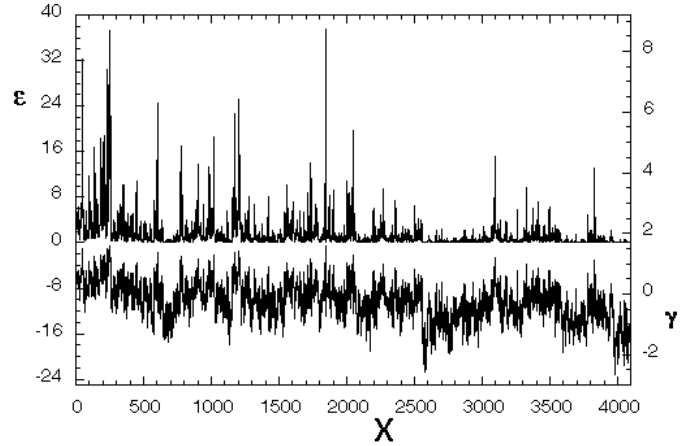


Fig. 3. A sample of a log-normal discrete cascade with total scale ratio 2^{12} . The generator γ (a correlated Gaussian noise) and the multifractal field ϵ are shown.

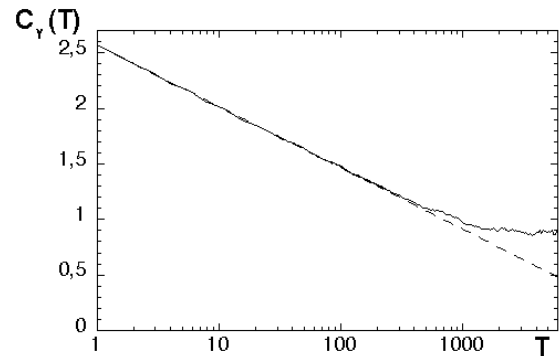


Fig. 4. The autocorrelation function of the generator, estimated from 100 realizations of a discrete log-normal cascade with $\mu = 0.25$. As expected this shows a logarithmic decrease over the whole scaling range. Dotted line: predicted logarithmic decay of the form $-\mu \log T$.

the resulting field for the cascade process ϵ and the singularity γ . It is visible that ϵ is highly intermittent while γ is a correlated noise. This correlation is illustrated in Fig. 4, showing $C_\gamma(\tau)$ versus $\log \tau$: the logarithmic decay is extremely well verified for almost 3 orders of magnitude, with a slope of about 0.24, close to the predicted value, which is $\sigma^2 / \log 2 = \mu$. Figure 5 represents the power spectrum of γ and of ϵ in log-log plot. These are both scaling, with respectively theoretical slopes of -1 and $-1 + \mu$; see Eq. (12) and the Fourier transform of Eq. (7). Experimental results are very close to theoretical power laws for the whole range of scales considered.

Figure 6 is a direct test of the scaling of the resulting field, for various order of moments: 100 realizations (each of length 4096) have been taken into account for the estimation of statistical moments. The dressed moments are represented in log-log plot, for different values of q ; the straight lines confirm a scaling law of the form given by Eq.5 for the dressed field. The slope of these straight lines give experimental estimates of $K(q)$, and the result-

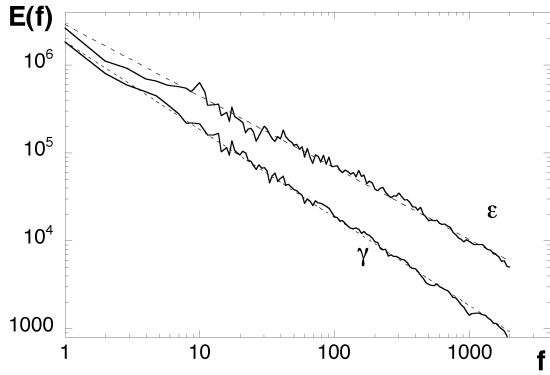


Fig. 5. The Fourier power spectrum of 100 realizations of a discrete log-normal multifractal field and of its generator. As expected, over the whole scaling range, the generator displays an exactly f^{-1} power spectrum, and the multifractal field a $f^{\mu-1}$. Dotted lines provide theoretical behaviours.

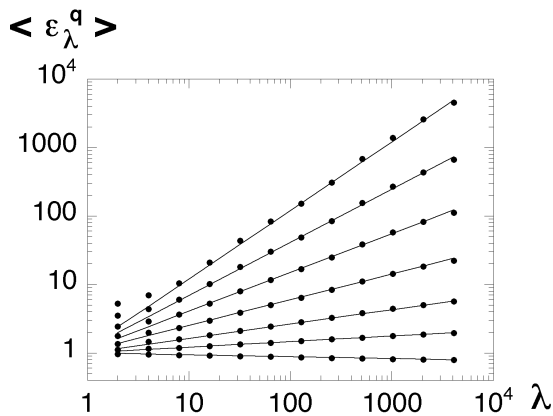


Fig. 6. The scaling of the moments of order 0.5, 1.5, 2, 2.5, 3, 3.5, and 4 (from below to above), estimated for 100 realizations of the discrete log-normal multifractal cascade. The different straight lines indicate the accuracy of the scaling property. The slopes of these straight lines give estimates of $K(q)$.

ing curve is shown in Fig. 7, compared to the theoretical bare expression $\frac{\mu}{2}(q^2 - q)$. There is an excellent agreement until a critical moment $q_s \approx 2.4$, above which the estimated function is linear: this corresponds to a maximum order of moment that can be estimated with a finite number of samples, since there are not enough realizations for an accurate estimation of the scaling exponent corresponding to larger order of moments. This may also correspond to the critical moment above which moments of the dressed field diverge; in this case experimental estimates are not infinite, but the exponent $K(q)$ becomes linear (see [56] for a discussion on bare/dressed exponents in an experimental context). In any case, experimental analysis shows that the simulated field has scaling moments, and as expected for low orders of moments, the moment function is close to the theoretical bare curve.

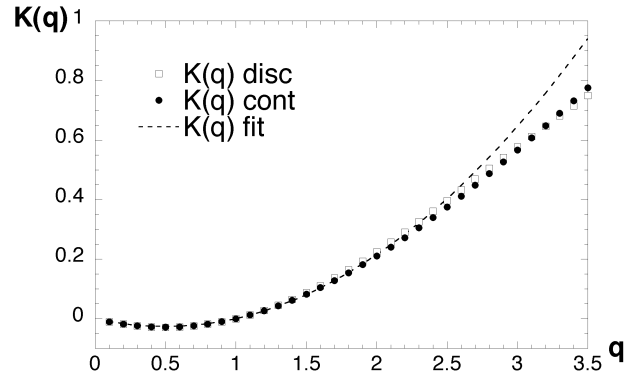


Fig. 7. The $K(q)$ function estimated from 100 realizations of the discrete multifractal simulation (open squares), from 106 points of a continuous simulation (filled dots), compared to the theoretical curve given by Equ. (17) (dotted line). There is an excellent agreement until a critical moment corresponding to the maximum moment that can be accurately estimated with a finite sampling.

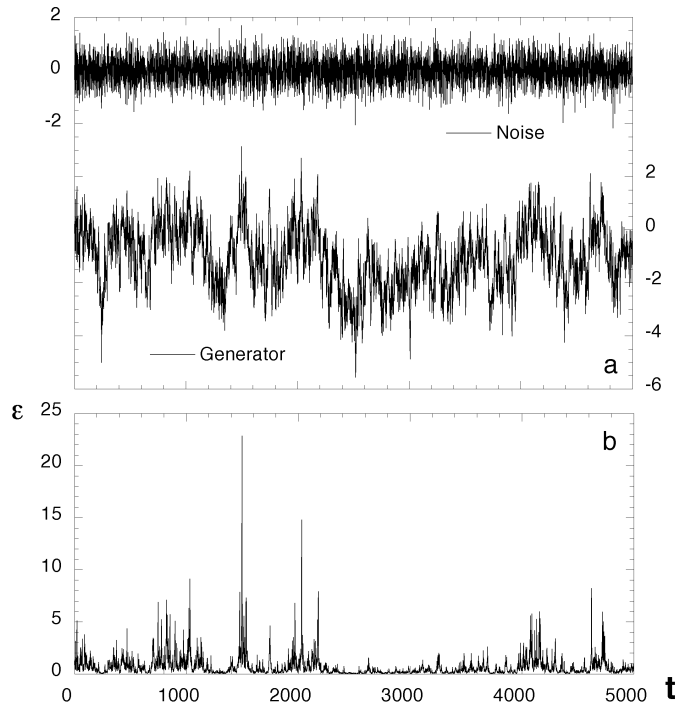


Fig. 8. (a) A sample of the Gaussian noise and of the generator; the generator is a moving average over the past of the noise, and corresponds to a correlated Gaussian noise. (b) A sample of the multifractal process, corresponding to the exponential of the generator of Fig. (8a).

3.2 Simulation of continuous and causal log-normal processes

Here we provide a stochastic simulation of the process given by Eq. (16), choosing $\lambda = 5,000$ and $\mu = 0.25$. This is done sequentially, generating the noise and a moving average over this noise. An arbitrary large number of points can be generated with this equation. We represent

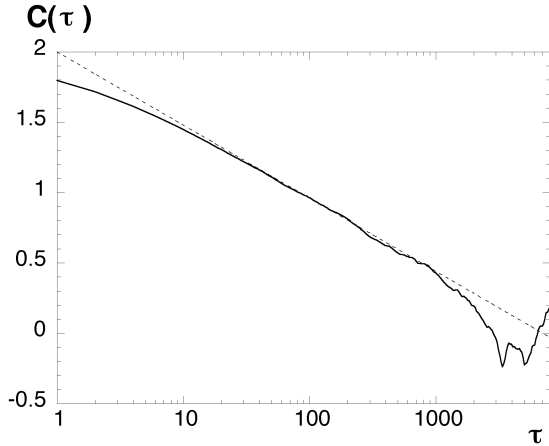


Fig. 9. The autocorrelation function of the generator, estimated from a continuous stochastic process with $\mu = 0.25$. As expected this shows a logarithmic decrease for large time lags. Dotted line: predicted logarithmic decay of the form $-\mu \log T$ with an experimental μ value of 0.23.

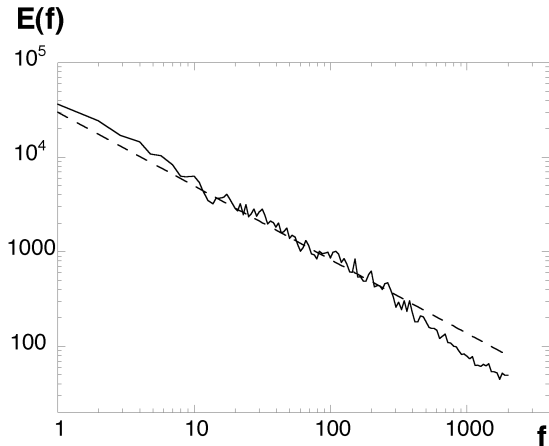


Fig. 10. The Fourier power spectrum of the continuous stochastic process. As expected, over the whole scaling range the multifractal field displays a $f^{\mu-1}$ regime with an experimental value of $\mu = 0.23$ (dotted line).

in Fig. 8a-b a sample path of 5,000 points for the process and its generator: Fig. 8a shows the Gaussian uncorrelated noise, together with the generator process, which is a moving average over this noise (with a specific kernel). This correlated noise has the same visual aspect as the generator obtained in Fig. 3 for discrete cascades. Figure 8b shows the field ϵ itself (the exponential of the generator): it presents as expected a huge intermittency.

To estimate the statistics of the path, we have generated 10^6 points. The scaling of their power spectra, together with their correlation properties, have been verified. The logarithmic decay of the autocorrelation function of the singularity process is shown in Fig. 9: it is nicely verified with a parameter of $\mu = 0.23$ close to the theoretical value. For short time lags (smaller than about 10) the experimental curve leaves the straight dotted line corre-

sponding to the fit; this is expected since the logarithmic decay was shown to be an asymptotic law for large enough time lags. Figure 10 shows the power spectrum of the field ϵ which is scaling with a fit of the form $f^{\mu-1}$ as expected, with an exponent of -0.77 , close to the expected value. The resulting moment function $K(q)$ is also shown in Fig. 7, as a comparison with the theoretical expression and the function estimated for the discrete simulation. The value corresponding to the continuous simulation is very close to previous results for the discrete simulation, and the same comments about bare/dressed scaling exponents apply. These different results confirm the different asymptotic expressions given for $1 \ll \tau \ll \lambda$ and the multifractal properties of the stochastic simulation.

4 Concluding comments

We have explored here the statistical properties of time series generated by a continuous and causal stochastic equation taking the form of the exponential of a stochastic integral. We have first shown that such generating equation indeed corresponds to a log-normal multifractal: this was verified with one point and two points statistics, either analytically and also numerically, in the asymptotic regime (for large enough time lags). We have also shown the composition rule of such equation, and considered its differential properties. This equation depends on 2 parameters: the intermittency parameter μ and the total scale ratio λ . For a fixed time and a variable scale ratio parameter, another type of process is obtained; the differential with respect to scale parameter leads to a Langevin equation for the logarithm of the process. We have linked this approach to experimental results about Langevin equations for the dissipation in turbulence. Of course, this does not indicate that log-normal cascades are the best models for turbulent intermittency. This is rather the exploration of an important and classical multifractal model; other continuous multifractals are associated to more complex generating equations having less straightforward differential properties.

This equation for log-normal multifractals is nevertheless believed to be of great interest since a quite simple stochastic equation generates a causal and continuous multifractal process, that can be used as a rather realistic approximation for various applications. It is also the first explicit continuous equation of its kind. This approach is finally believed to open the door to many interesting generalizations, including cascades of matrices using a stochastic continuous product framework, which is only quickly evoked here.

Acknowledgement

We thank L. Coutin and D. Marsan for useful discussions, and the referees for their useful suggestions.

Appendix A. Characteristic functions and infinitely divisible distributions

We recall here some useful properties of characteristic functions, infinitely divisible distributions, Gaussian and Lévy-stable random variables. Useful references for these topics are Feller [10], Janicki and Weron [57], and Samorodnitsky and Taqqu [58].

Let X be a random variable with probability density $p(x)$. The usual characteristic function is the Fourier characteristic function $\phi(k)$ defined as

$$\phi(k) = \langle e^{ikx} \rangle \quad (48)$$

Since when studying multiplicative cascades real moments are introduced, we use here Laplace characteristic functions, assuming that the positive tail of the probability density decreases fast enough for the integral to converge:

$$f(q) = \langle e^{qx} \rangle = \int_{-\infty}^{+\infty} e^{qx} p(x) dx \quad (49)$$

One thus have $f(q) = \phi(-iq)$ where $\phi(q)$ are given in the usual tables of characteristic functions.

Infinite divisibility is a property that has no simple expression for probability densities. Instead, this property is very simply characterized using characteristic functions. A probability distribution is said to be infinitely divisible (ID) if its characteristic function f has the following property: for any n integer, there exist a characteristic function f_n such that:

$$f_n^n = f \quad (50)$$

In such a case one can introduce the second characteristic function $\Psi = \log f$:

$$\Psi(q) = \log \langle e^{qx} \rangle \quad (51)$$

Let us consider a second characteristic function $\Psi(q)$. If for any $a > 0$, $a\Psi(q)$ is still a second characteristic function, then the distribution associated to $\Psi(q)$ is ID.

Let us give two examples: a Poisson distribution with mean α has a second characteristic function of

$$\Psi(q) = \alpha(e^q - 1) \quad (52)$$

Lévy-stable random variables can be defined as follows: let $(X_i)_{i=1..n}$ be independent random variables of the same law, and n any integer. Then the law is stable if there exists $a_n > 0$ and b_n such that $a_n \sum_{i=1}^n X_i - b_n$ has the same law as the X_i . Strictly stable random variables are the ones for which $b_n = 0$, corresponding to centered $\langle X_i \rangle = 0$ variables. Using the second characteristic function, it is easily seen that Lévy random variables, for which

$$\Psi(q) = \Gamma^\alpha q^\alpha \quad (53)$$

are stable with $a_n = n^{1/\alpha}$. The parameter $\Gamma > 0$ is called the scale or dispersion parameter; it plays the same role as the variance for gaussian random variables: for $\alpha = 2$,

one recovers gaussian random variables with $\sigma^2 = \Gamma^2/2$. Lévy-stable random variables are characterized by the basic parameter α , limited to the range $0 \leq \alpha \leq 2$. One may note that Lévy-stable variables can take high values with hyperbolic probability tails, so that for the Laplace characteristic function to converge, one must consider only skewed Lévy variables, for which the hyperbolic tail corresponds to negative values only. In this case, the Laplace characteristic function is defined for moments $q > 0$.

Appendix B. Stable stochastic integrals

A useful reference for this topic is e.g. Janicki and Weron [57]. The rescaling properties of stable random variables can be used to define stable stochastic integrals. Let us consider again $Y = \sum_{i=1}^n X_i$, where $(X_i)_{i=1..n}$ are independent strictly stable random variables having the same law, with parameters α and Γ_x . Then one has $\Psi_Y(q) = n\Psi_x(q) = n\Gamma_x^\alpha q^\alpha$ showing that:

$$\Gamma_y = n^{1/\alpha} \Gamma_x \quad (54)$$

This property can be used to build stable random measures and in a consistent way, stable stochastic integrals.

For an interval of width dx , $M(dx)$ is defined as a strictly stable random measure, i.e. a strictly stable random variable of index α and of scale parameter $\Gamma_M = (dx)^{1/\alpha}$. It has the following second characteristic function:

$$\Psi_M(q) = (\Gamma_M q)^\alpha = q^\alpha dx \quad (55)$$

For a positive valued function F , such that $\int_a^b F^\alpha(x) dx$ exists, the stochastic integral $I = \int_a^b F(x) M(dx)$ is a random variable defined as follows: it is the strictly stable random variable of scale parameter

$$\Gamma_I = \left(\int_a^b F^\alpha(x) dx \right)^{1/\alpha} \quad (56)$$

which can be rewritten in the following way, using its second Laplace characteristic function:

$$\log \langle e^{q \int_a^b F(x) M(dx)} \rangle = \left(\int_a^b F^\alpha(x) dx \right) q^\alpha \quad (57)$$

This fully characterizes stable stochastic integrals. In particular, for $\alpha = 2$, the Gaussian stochastic integral $I = \int_a^b F(x) dB(x)$ is still a Gaussian random variable with the variance

$$\sigma_I^2 = \int_a^b F^2(x) dx \quad (58)$$

Gaussian stochastic integrals have also the property:

$$\langle \int_{E_1} F(x) dB(x) \int_{E_2} G(x) dB(x) \rangle = \int_{E_1 \cap E_2} F(x) G(x) dx \quad (59)$$

Indeed, if $E_1 \cap E_2 = \emptyset$ the two integrals and independent random variables and whenever $E_1 \cup E_2 \neq \emptyset$ only the intersection contributes to the correlation.

Let us finally consider the stochastic process defined as:

$$W_K(t) = \int_0^t K(t, s) dB(s) \quad (60)$$

where the kernel K possesses some regularity conditions:

$$K(t, s) = 0; \quad s > t \quad (61)$$

$$\int_0^T \left(\int_0^u \partial_t K(u, s)^2 ds \right)^{1/2} + \int_0^T K^2(s, s) ds < \infty \quad (62)$$

then $W_K(t)$ is a semimartingale with respect to the usual filtration and has the following representation

$$dW_K(t) = K(t, t)dB(t) + W_{\partial_t K}(t)dt \quad (63)$$

See for more details Carmona and Coutin [59].

Appendix C. Stochastic continuous product

Stochastic multiplicative integrals or continuous products have been introduced in the field of continuous martingales (see McKean [46], and developed by e.g. Ibero [47], Doleans-Dade [48], Emery [49] and also Karandikar [60]). Below we propose a personal and short didactic introduction to such objects.

Infinitely divisible distributions are naturally associated to random measures, which can also be called random additive set function. The discrete addition of ID random variables, when densified, leads to stochastic integrals. The same way, one wants here to densify a discrete multiplication of random variables, to obtain a continuous product. This can be done introducing random multiplicative set functions (RMSF). We associate with a measure $m(A)$ for a set $A \neq \emptyset$, a multiplicative set function $n(A)$ defined as $n(A) = e^{m(A)}$. Then for A and B such that $A \cap B = \emptyset$, one has $n(A \cup B) = n(A)n(B)$. A random multiplicative set function N can then be defined for a set A : $N(A) = e^{M(A)}$ and is characterized by the control measure $m(A)$. It is clear that for A and B with a void intersection, one has multiplicative random variables: $N(A \cup B) = N(A)N(B)$.

This is useful to introduce a random continuous product. Let us take non-intersecting intervals A_i and introduce the random variable P :

$$P = \prod_{i=1}^n N(A_i) \quad (64)$$

This can be generalized to a continuous limit, taking intervals of the form $A_i = [a + i \frac{b-a}{n}, a + (i+1) \frac{b-a}{n}]$, whose

reunion is the interval $[a, b]$ and whose width decreases with n . This way one has the limit:

$$\bigcap_a^b N(dx) = \lim_{n \rightarrow \infty} \prod_{i=0}^{n-1} N \left(\left[a + i \frac{b-a}{n}, a + (i+1) \frac{b-a}{n} \right] \right) \quad (65)$$

One obtains a stochastic continuous product, as the limit of a product of random multiplicative set functions, noted \bigcap . It has the following basic property:

$$\left\langle \left(\bigcap_A N(dx) \right)^q \right\rangle = e^{m(A)\Psi_0(q)} \quad (66)$$

which can be used for continuous cascades ($\Psi_0(q)$ is a reference second Laplace characteristic function).

References

1. L. F. Richardson, *Weather Prediction by Numerical Process* (Cambridge University Press, 1922).
2. A. N. Kolmogorov, C. R. Acad. Sci. URSS **30**, 301 (1941).
3. G. K. Batchelor and A. A. Townsend, Proc. Roy. Soc. A **199**, 238 (1949).
4. A. N. Kolmogorov, J. Fluid Mech. **13**, 82 (1962).
5. A. M. Obukhov, J. Fluid Mech. **13**, 77 (1962).
6. A. S. Gurvich, S. L. Zubkovski, Izv. Akad. Nauk. SSSR, Ser. Geofiz., 1856 (1963).
7. S. Pond, R. W. Stewart, Izv. Akad. Nauk. SSSR, Ser. Fis. Atmosf. Okeana **1**, 914 (1965).
8. U. Frisch, *Turbulence; the legacy of A. N. Kolmogorov* (Cambridge University Press, Cambridge, 1995) 296 pp.
9. A. M. Yaglom, Sov. Phys. Dokl **11**, 26 (1966).
10. W. Feller, *An Introduction to Probability Theory and its Applications, vol. II*, 2nd edn. (Wiley, New York 1971).
11. B. B. Mandelbrot, J. Fluid Mech. **62**, 331 (1974).
12. J.-P. Kahane and J. Peyriere, Adv. Math. **22**, 131 (1976).
13. M. E. Cates, J. M. Deutsch, Phys. Rev. A **35**, 4907 (1987).
14. D. Marsan, D. Schertzer, S. Lovejoy, J. Geophys. Res. **101**, 26333 (1996).
15. B. B. Mandelbrot and Van Ness, SIAM Rev. **10**, 422 (1968).
16. A. Arneodo et al., Phys. Rev. Lett. **80**, 708 (1998).
17. A. Arneodo, E. Bacry and J.-F. Muzy, J. Math. Phys. **39**, 4142 (1998).
18. D. Schertzer, S. Lovejoy, J. Geophys. Res. **92**, 9693 (1987).
19. D. Schertzer, S. Lovejoy, in *Scaling, fractals and non-linear variability in geophysics*, edited by D. Schertzer and S. Lovejoy (Kluwer, Berlin, 1991), p. 41.
20. J.-F. Muzy, J. Delour, E. Bacry, Eur. Phys. J. B **17**, 537 (2000).
21. E. Bacry, J. Delour, J.-F. Muzy, Phys. Rev. E **64**, 026103 (2001).
22. Z.-S. She, E. Waymire, Phys. Rev. Lett. **74**, 262 (1995).
23. D. Schertzer, et al., Fractals **5**, 427 (1997).
24. F. Schmitt, S. Vannitsem, A. Barbosa, J. Geophys. Res. **103**, 23181 (1998).
25. Y. Saito, J. Phys. Soc. Japan **61**, 403 (1992).
26. E. A. Novikov, Phys. Rev. E **50**, R3303 (1994).
27. B. Castaing, J. Phys. II France **6**, 105 (1996).
28. F. G. Schmitt, *Intermittence et turbulence*, Habil. Dir. Rech Thesis (U. Paris 6, 2001).

29. F. G. Schmitt, D. Marsan, Eur. Phys. J. B **20**, 3 (2001).
30. J.-F. Muzy, E. Bacry, Phys. Rev. E **66**, 056121 (2002).
31. P. Chainais, R. Riedi, P. Abry, in *Proceedings of the Conference on Physics, Signal and Image Processing* (Grenoble, 2003).
32. B. Rajput, J. Rosinski, J. Prob. Th. Rel. Fields **82**, 451 (1989).
33. J. Barral, B. B. Mandelbrot, J. Prob. Th. Rel. Fields, in press (2003).
34. J. Cleve and M. Greiner, Phys. Lett A **273**, 104 (2000).
35. B. Castaing and B. Dubrulle, J. Phys. II France **5**, 895 (1995).
36. Y. Malecot, et al., Eur. Phys. J. B **16**, 549 (2000).
37. B. Castaing, Y. Gagne and E. Hopfinger, Physica D **46**, 177 (1990).
38. B. Castaing, in *Scale invariance and beyond*, edited by B. Dubrulle, F. Graner, D. Sornette (Les Houches, EDP Sciences, Springer, 1997).
39. P.-O. Amblard and J.-M. Brossier, Eur. Phys. J. B **12**, 579 (1999).
40. R. Friedrich, J. Peinke, Phys. Rev. Lett. **78**, 863 (1997).
41. A. Naert, R. Friedrich and J. Peinke, Phys. Rev. E **56**, 6719 (1997).
42. C. Renner, J. Peinke and R. Friedrich, J. Fluid Mech. **433**, 383 (2001).
43. P. Marcq, A. Naert, Physica D **124**, 368 (1999).
44. F. Schmitt, et al., Phys. Rev. Lett. **68**, 305 (1992).
45. J. D. Dollard and C. N. Friedman, *Product Integration with Applications to Differential Equations* (Addison-Wesley, London, 1979).
46. H. P. McKean, Jr., Mem. Coll. Sci. Kyoto Univ. **33**, 25 (1960).
47. M. Ibero, M., Bull. Sc. math. **100**, 175 (1976).
48. C. Doleans-Dade, Z. W-theorie **36**, 93 (1976).
49. M. Emery, M., Z. Wahrsch. verw. **41**, 241 (1978).
50. U. Frisch, P.-L. Sulem and M. Nelkin, J. Fluid Mech. **87**, 719 (1978).
51. S. Tavoularis and S. Corrsin, J. Fluid Mech. **104**, 311 (1981).
52. R. A. Antonia, L. Djenidi and P. R. Spalart, Phys. fluids **6**, 2475 (1994).
53. C. G. Speziale and T. Gatski, J. Fluid Mech. **344**, 155 (1997).
54. S. Pope, *Turbulent flows* (Cambridge University Press, 2000).
55. A. Arneodo, et al., Europhys. Lett. **34**, 411 (1996).
56. F. Schmitt, D. Schertzer, S. Lovejoy, Y. Brunet, Nonlin. Proc. Geophys. **1** 95 (1994).
57. A. Janicki, A. Weron, *Simulation and chaotic behavior of α -stable stochastic processes* (Marcel Dekker, New York, 1994) 355 pp.
58. G. Samorodnitsky, M. S. Taqqu, *Stable non-Gaussian random processes : stochastic models with infinite variance* (Chapman & Hall, New York, 1994) 632 pp.
59. P. Carmona and L. Coutin, C. R. Acad. Sci Paris serie I **330**, 231 (2000).
60. R. L. Karandikar, in *Prediction theory and harmonic analysis*, edited by V. Mandrekar and H. Salehi (North Holland, 1983), p. 191.